Proceedings of the European Conference "Physics of Magnetism" (PM'08), Poznań 2008

Hyperfine Interactions of ^{57}Fe in Pt_3Fe — *Ab Initio* and Mössbauer Effect Studies

J. Deniszczyk[a], D. Satuła[b], J. Waliszewski[b], K. Rećko[b], W. Olszewski[b], G. Parzych[c] and K. Szymański[b]

[a]Institute of Materials Science, University of Silesia
Bankowa 12, 40-007 Katowice, Poland

[b]Faculty of Physics, University of Białystok
15-424 Białystok, Poland

[c]Ks. Anny 7/54, 18-404 Łomża, Poland

The Mössbauer effect and *ab initio* investigations of an electric field gradient at ^{57}Fe nuclei in Pt_3Fe compound are presented. It is shown that nonzero ^{57}Fe electric field gradient exists in the cubic Pt_3Fe. *Ab initio* study of Pt_3Fe in antiferromagnetic state confirms the presence of electric field gradient at ^{57}Fe nuclei. Lattice, local valence electron ($3d$, $4p$) and weakly bound $3p$ core electron contributions to electric field gradient are separated out and discussed in the context of the electronic structure changes upon the antiferromagnetic phase transition.

PACS numbers: 71.15.Ap, 71.15.Nc, 71.20.–b, 71.20.Be, 71.20.Lp, 75.50.Bb, 76.80.+y

1. Introduction

The ordered Pt_3Fe alloy of cubic Cu_3Au ($L1_2$) structure shows an antiferromagnetic (AFM) phase transition at $T_N = 150$ K [1] displaying the magnetic order of $\left(\frac{1}{2}, \frac{1}{2}, 0\right)$-type ($AFM_2$) at high and of $\left(\frac{1}{2}, 0, 0\right)$-type ($AFM_1$) at lower temperatures [2]. The non-collinear magnetic structure in Pt_3Fe was also reported from low-temperature neutron diffraction data [3]. The compound was measured by the Mössbauer effect method [4] but no information on the electric field gradient (EFG) tensor was reported. The electronic structure of Pt_3Fe was calculated by *ab initio* methods [5] but the hyperfine interaction parameters were not given. We present a complete, Mössbauer effect and *ab initio*, study of Pt_3Fe compound. The aim of band structure calculations was to elucidate the physical mechanism responsible for the occurrence of the EFG at the ^{57}Fe nuclei in AFM Pt_3Fe. With this aim the *ab initio* electronic structure calculations for Pt_3Fe were carried out for paramagnetic (NM), ferromagnetic (FM) and both AFM ground states. The ^{57}Fe hyperfine parameters were determined and compared with the experimental data.

2. Investigation details

The samples were prepared by arc melting from platinum, natural iron and ^{57}Fe isotope, with the ratio of ^{57}Fe to natural Fe equal to 0.22 for the first sample and 0.99 for the second. The first one, after homogenization of the ingot (56 h at 1150 K), was powdered and then annealed in the vacuum by heating to 1280 K and cooling gradually from 1180 K at the rate 0.35 K/h for 236 h. The absorber of 19 mg/cm^2 thick was prepared. The second sample, homogenized during 12 h at 1200 K, was made in the form of foil with average thickness of 12.4 mg/cm^2. Final annealing of the foil was similar as for the powders. The Mössbauer effect measurements were performed in constant acceleration mode and the ^{57}Co isotope in Cr matrix was used as a source of ^{57}Fe resonant radiation.

The electronic structure calculations were performed with the use of the WIEN2k code [6] employing the general potential linear augmented plane wave (FP-LAPW) method within the density functional theory (DFT) formalism. The gradient corrected local spin density approximation form of the exchange correlation potential given in [7] was used. The core electron states were partitioned into strongly bound true core states (Fe: $1s$–$2p$, Pt: $1s$–$4d$), which were treated atomic-like in the spherical *all-electron* muffin-tin (MT) potential, and weakly bound semicore states (Fe: $3sp$, Pt: $4f$ and $5sp$) considered as local orbitals (LO) [8] and treated as band-like states in the *full potential* with no shape approximation. For the true core states, the fully relativistic DFT formalism was employed, while the other states were solved within the scalar-relativistic approximation neglecting the spin–orbit interaction. For all studied phases the MT radii of 2.2 a.u. for Fe and 2.4 a.u. for Pt were chosen. The set of the $\boldsymbol{k}$ vectors and the values of RK_{max} factor were chosen to gain the total energy precision of 10^{-6} Ry

and the EFG relative error less than 1%. All calculations were performed for the experimental lattice parameters. The EFG tensor was calculated using the formula derived by Weinert [9] for the shape model of periodic charge distribution used in the FP-LAPW method. The formula divides the EFG in contribution of electrons located inside MT sphere (local EFG) and the part dependent on the charge distributed outside the MT sphere, called lattice EFG [10]. In our calculations the contribution to EFG of true core states is omitted but, as argued in [10], it is negligible in metals.

3. Results and discussion

The room temperature X-ray measurements reveal the single $L1_2$ phase for both samples and the lattice parameter was found as 0.3868(1) nm (powder) and 0.3871(1) nm (foil), in agreement with the data presented in [1, 2]. The diffraction pattern did not exhibit the c/a distortion with the accuracy of 10^{-5}. The Mössbauer spectra were analyzed within the transmission integral approach. Because the local atomic environment of Fe atom in Pt_3Fe is of cubic symmetry firstly we have fitted a Zeeman sextet to the experimental spectra. The fitted function is shown in Fig. 1a (solid line). The difference between experimental spectrum and the fitted function clearly shows the shift of outer doublet with respect to the inner quartet which indicates the presence of the quadrupolar splitting (QS) of the Zeeman sextet. To exclude the drive nonlinearity as a possible reason of the line shift we performed fits on calibration spectrum of α-Fe treating QS in the same way as used in Fig. 1. The fits of the same quality for $QS = 0$ and QS treated as free parameter were found. In both cases the shift of lines was zero with the uncertainty one order of magnitude smaller than the QS found in Pt_3Fe which excludes drive nonlinearity as the possible reason of deviations shown in Fig. 1a. With this in mind another fit for Pt_3Fe was performed with the QS taken into account. Assuming a nonzero EFG at Fe nucleus a good quality fit was obtained (solid line in Fig. 1b) with the QS values of $-0.038(7)\frac{\text{mm}}{\text{s}}$ for the ground state, independent of the sample preparation. We obtained the magnitude of magnetic hyperfine field consistent with that reported in [2, 4].

Our calculations give the ground state band structure (Fig. 2) and magnetic properties of Pt_3Fe in NM, FM and AFM_1 phases similar to that reported in [5]. The magnetic moment of Fe (3.23 μ_B in FM state) enhances slightly in AFM state (AFM_1: 3.27 μ_B, AFM_2: 3.24 μ_B). The magnetic moment of Pt (0.37 μ_B in FM state) disappears in the AFM_2 state while in the AFM_1 state the Pt atoms located in the ferromagnetically ordered planes have the magnetic moment of 0.15 μ_B parallel to plane magnetization. The Pt atoms surrounded by two pairs of Fe magnetic moments of opposite polarization are not polarized. Calculations have shown that the transition from FM state to either AFM state does not change the

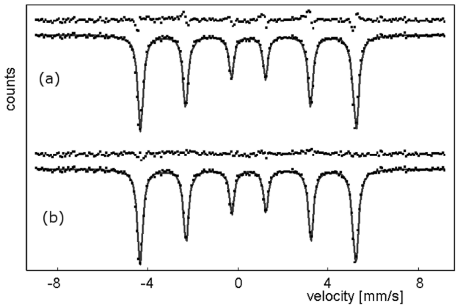

Fig. 1. Mössbauer spectrum of ordered Pt_3Fe measured at $T = 13$ K and fitted function with only magnetic dipolar (a) and both magnetic dipolar and electric quadrupolar interactions (b) taken into account. Solid lines show the fitted function.

MT charges by more than ≈ 0.005 electrons. This effect and the fact that the crystal structure does not change upon the FM $\rightarrow$ AFM phase transition means that the lattice source of EFG is not effective in AFM Pt_3Fe and the question emerges as to the source of the QS we observe in the AFM Pt_3Fe. We claim that the asymmetry of the valence electron charge distribution, which occurs in AFM state, is the dominant source of the EFG in AFM Pt_3Fe.

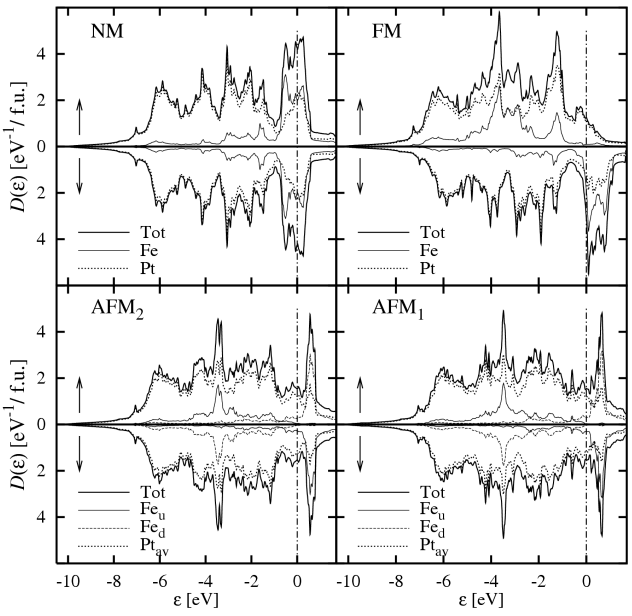

Fig. 2. The Pt_3Fe total density of states per spin direction with separated atomic contributions, calculated in paramagnetic (NM), ferromagnetic (FM) and two antiferromagnetic (AFM_1, AFM_2) phases. The Fe_u and Fe_d denote Fe atoms with opposite spin moment orientation. The vertical dash-dot line indicates the Fermi level.

The band structure of Pt_3Fe is dominated by the hybridizing Pt $5d$ and Fe $3d$ states (Fig. 2). In the NM state the anti-bonding band of hybridized Fe $3d$ and Pt $5d$

states forms at the Fermi level (ε_F). Upon the phase transition to the FM state the exchange interaction results in the shift of the majority spin Fe 3*d* band far below ε_F with simultaneous reconstruction of 3*d* orbital energy location. As an effect almost complete occupation of these bands is reached. The minority spin anti-bonding states (3*d* and 5*d*) shift above the ε_F leaving the bottom edge of the band crossing the Fermi level. The crystal-field splitting of Fe 3*d* states has effect in the different magnitude of minority spin density of states $D(\varepsilon_F)$ with 3*d*–e_g and 3*d*–t_{2g} symmetry. The transition to the AFM state does not change the width and exchange splitting of the valence band, but some important changes in the Fe 3*d* band structure can be observed. The majority spin states accumulate in the bonding energy region (≈ -4 eV) and hybridize strongly with the 5*d* states of Pt. The anti-bonding band of minority spin 3*d* states narrows and shifts above the ε_F. The lowering of the site symmetry of Fe position in AFM state ($4/mmm$) lifts partially the degeneracy of 3*d*–t_{2g} and 3*d*–e_g states. Interband charge transfer between the split 3*d* states of Fe results in the asymmetry in partial state population. The effect is significant mainly for minority spin states where approximately 0.24 electrons change their orbital character from t_{2g} to the e_g-type which leads to the enhancement of the population of $3d_{z^2}$ orbital and consequently of electronic charge distribution along the z axis. The change of the character of the 3*d*–5*d* majority spin band hybridization and changes in the population of the minority spin Fe 3*d* orbitals generate the EFG at Fe nuclei in AFM Pt_3Fe.

TABLE

Magnetic hyperfine field (B_{hf}) and main component of electric field gradient (ϑ_{zz}) with separated partial contributions. The $\vartheta_{zz}^{exp.}$ was estimated for 14.41 keV ^{57}Fe nuclear excitation, assuming the asymmetry parameter equal to zero and nuclear quadrupole moment of ^{57}Fe equal to 0.17 10^{-28} m^2 [11].

	B_{hf}	Lattice	ϑ_{zz} [10^{21} V m^{-2}]			
	[T]		3*p*-cor.	4*p*-val.	3*d*-val.	Total
FM	25.6	–	–	–	–	–
AFM_1	16.2	−0.001	−0.29	0.03	2.12	1.85
AFM_2	18.7	0.003	0.13	−0.02	−0.62	−0.5

Experimental ϑ_{zz}: -0.21×10^{21} V m^{-2} at $T = 13$ K.

The calculated hyperfine parameters in Pt_3Fe are collected in Table and compared with the experimental data. The analytic formula of Weinert for the main component (ϑ_{zz}) of the diagonal EFG allows analysis of separate contributions of states located at different regions of energy scale and for different electronic orbital quantum numbers. In agreement with calculations for metals reported in [10] we found that the lattice (ϑ_{zz}) is minutely small. The dominant contribution to ϑ_{zz} at Fe nuclei comes from the 3*d*-type valence electrons cancelled partially by weakly bound 3*p* core electrons due to *shielding effect*. The contribution of valence Fe 4*p* states is negligible. For both AFM phases the calculated asymmetry parameter is equal to zero.

4. Conclusions

Our *ab initio* study shows that the AFM transition in Pt_3Fe forces the local valence and weakly bound core electron charge density reordering which lowers the local charge density symmetry and is responsible for the occurrence of the electric field gradient at Fe nuclei in the AFM Pt_3Fe. The ϑ_{zz} is dominated by the 3*d* electron contribution, the *lattice* part is negligible. Some *shielding effect* of Fe 3*p* states is observed. The ϑ_{zz} calculated for AFM_2 phase is close to the experimental one at low temperature, which disagrees with experimentally based conclusion that the AFM_1-type of order realizes in the ground state of Pt_3Fe. The disagreement can originate from the noncollinear magnetic order and spin–orbit interaction, neglected both in our calculations.

Acknowledgments

The work was partially supported as a research project by the funds allocated for scientific research in years 2008–2011.

References

[1] J. Crangle, *J. Phys. (France)* **20**, 435 (1959).

[2] G.E. Bacon, J. Crangle, *Proc. R. Soc. A* **272**, 387 (1963).

[3] S. Yano, Y. Tsunoda, *J. Magn. Magn. Mater.* **319**, 1841 (2007).

[4] P. Steinbach, R.A. Brand, W. Keune, *J. Magn. Magn. Mater.* **70**, 102 (1987).

[5] M. Podgórny, *Phys. Rev. B* **43**, 11300 (1991).

[6] K. Schwarz, P. Blaha, G.K.H. Madsen, *Comp. Phys. Commun.* **147**, 71 (2002).

[7] J.P. Perdew, K. Burke, M. Ernzerhof, *Phys. Rev. Lett.* **77**, 3865 (1996).

[8] D. Singh, *Plane Waves, Pseudopotentials and the LAPW Method*, Kluwer Academic, Boston 1994.

[9] M. Weinert, *J. Math. Phys.* **22**, 2433 (1981).

[10] P. Blaha, K. Schwarz, P.B. Dederichs, *Phys. Rev. B* **37**, 2792 (1988).

[11] U.D. Wdowik, K. Ruebenbauer, *Phys. Rev.* **76**, 155118 (2007).